Identification of Hub Genes and Key Pathways of Paraquat Induced Human Embryonic Pulmonary Fibrosis by Bioinformatics Analysis and Vitro Experiments

Yue Fu (drfuyue@Gmail.com)
First People's Hospital of Foshan
Xiang Xia Zeng
The Affiliated Hospital of Guangzhou Medical University
Jin Lun Hu
The First's People Hospital of Foshan
Mei Yan
The First's People Hospital of Foshan
CHun Ming Xie
The First People's Hospital of Foshan
Wei Gan XU
The First's People's Hospital of Foshan
Zi Cong Gu
The First's People Hospital of FOshan

Original research

Keywords: Paraquat, pulmonary fibrosis, bioinformatics analysis, vitro experiments

Posted Date: September 15th, 2020

DOI: https://doi.org/10.21203/rs.3.rs-73540/v1

Abstract

Background: Paraquat is highly toxic pesticide, which usually led to acute lung injury and subsequently develop pulmonary fibrosis, the exact mechanisms of PQ-induced lung fibrosis remain largely unclear and no specific drugs for this disease have been approved.

Methods: Our study aimed to identify its potential mechanism though modeling study in vitro and bioinformatics analysis. Gene expression datasets associated with PQ-induced lung fibrosis were obtained from the Gene Expression Omnibus and differentially expressed genes (DEGs) were identified using GEO2R. Functional enrichment analyses were performed using the Database for Annotation.

Results: The DEGs in the two datasets, of which 92 overlapping genes were found in two microarray datasets. Functional analysis demonstrated that the 92 DEGs were enriched in the 'TNF signaling pathway', 'CXCR chemokine receptor binding', and 'core promoter binding'. Moreover, nine hub genes were identified from a protein-protein interaction network.

Conclusions: This integrative analysis firstly identified candidate genes and pathways in PQ-induced lung fibrosis, as well as benefit to research novel approaches for treating for control of PQ-induced pulmonary fibrosis.

1. Introduction

Paraquat (N,N0-dimethyl-4,40-bipyridinium dichloride, PQ) has become a herbicide widely used in agriculture for its rapidly contact-dependent killing of broad leaf weeds and plants with non-selective characteristics(1, 2).Due to its potential danger to human health and livestock, PQ intoxication, which has become a common cause of pesticide poisoning deaths and resulted in a fatality rate of 38.08% in China(2).PQ intoxication leads to multiple organ damage especially in the lungs, which is characterized by severe pulmonary inflammation, edema, and epithelial cell destruction,pulmonary fibrosis is the most serious consequence caused by PQ intoxication, which related with high mortality and lacked of effective therapeutic strategy (3, 4).Moreover, due to the extremely high toxicity and lethality of PQ, that led to the study more difficultly and the underlying mechanism of PQ-induced pulmonary fibrosis remains unclear.Thus, it is of great importance and urgency to identify the highest non-lethal concentration of PQ-induced pulmonary fibrosis.

Microarray technology help to determinate mRNA profiles related to human disease and provides a comprehensive, unbiased approach to systematically analyze disease processes, including pulmonary fibrosis(5). Moreover, some studies have declared that PQ intoxication may alterate at the genome level(5–8). Accordingly, integrative analyses of genes and pathways associated with lung fibrosis may provide an insight into therapeutic targets and diagnostic biomarkers for PQ-induced pulmonary fibrosis.

The present study aimed to identify the highest non-lethal concentration of PQ-induced pulmonary fibrosis in vitro through testing collage I protein and α-SMA for further study. Moreover, we analyze differentially expressed genes (DEG) in the PQ intoxication, Hub genes were screened from a protein-protein interaction (PPI) network for the next study. This integrative analysis identified candidate genes and pathways in PQ intoxication and the highest non-lethal concentration of PQ-induced pulmonary fibrosis in vitro.

2. Materials And Methods

2.1 Establishment of Vitro studies

Human embryonic pulmonary fibrosis (MRC-5) were purchased from the cell bank of Institute for occupational diseases in Guangdong Province and cultured in DMEM supplemented with 10% (FBS, Invitrogen) 25 μg / ml penicillin and 25 μg / ml streptomycin (Invitrogen). All cells were incubated in a constant temperature cell incubator with 5% CO2 at 37 ℃. MRC-5 cells in logarithmic growth phase were digested to prepare single cell suspension, which was inoculated into 96-well culture plates with a density of 5 × 103 cells/well and cultured overnight at 37℃. PQ with concentrations of 50, 100, 150 and 200 μmol/L were selected for 24 h, 48 h and 72h,and PQ were not added as negative controls. 50 μL of MTT (5 g/L) solution was added to 96-well plates respectively, and the plates were incubated at 37℃ for 4 hours. After incubation, 150 μL DMSO solution was added to each well. Subsequently, add 72% of the medium volume of CCK-8 reagent after 72 h of culture, continue to incubate for 1 h, record the absorbance at 450 nm with a microplate reader, and draw the growth curve. The experimental protocol of this study was not necessary of ethical approval because our study was the vitro experiment.

2.2 Western blot analysis.

Western blot analysis was used to detect protein expression in the CollagenI,CollagenIII, SAM of lung tissue. The total protein (Sigma) in cell line was extracted according to the manufacturer's steps. All steps are carried out on ice to minimize degradation. The total protein concentration was determined by BCA protein assay kit (Bio-rad). The total protein was heated to 100℃ and incubated for 5 minutes, then SDS-polyacrylamide gel electrophoresis (120V, 100 min) was used. The protein isolated from the SDS gel was then transferred to the PVDF membrane (300 mA, 80 min). After the completion of membrane transfer, the target band was sealed with 5% TBS, Put the PVDF membrane into a small ziplock bag containing 3 ml horseradish peroxidase-labeled corresponding secondary antibody solution, and shake gently at room temperature for 50 min on a shaker; wash the PVDF membrane 3 times for 10 min with TBST; place the ECL kit in a dark room Medium A and B reagents were mixed in equal volumes in 1.5 ml EP tubes. After 1 min, the PVDF membrane protein incubated with the above antibodies was placed on the plastic wrap with the face up, and the mixed liquid was dropped on the membrane. After 1 min, Cover the PVDF film with plastic wrap and place it in a medical X-ray film holder. Place the X-ray film on the film, close the X-ray film holder, and start timing; adjust the time required for the exposure according to the strength of the signal, which usually ranges from a few seconds to a few minutes (you can also make a tablet time gradient To select the best effect film) Open the X-ray film holder, take out the film, quickly immerse it in the developing solution to develop, after the obvious band appears, transfer the film to clean water and wash it, then transfer to the fixing solution to terminate development.

2.3 RT-PCR.

Total cellular RNA was extracted following the kit instructions (Thermo, shenzhen, China) and UV spectrophotometry was used to determine the RNA quality and concentration in the samples. RNA was synthesized into cDNA by a reverse transcription reaction for later PCR amplification. The primers used for the internal control SMA were: forward, CCTTGAGAAGAGTTACGAGTTG and reverse, TGCTGTTGTAGGTGGTTTCA; amplification length, 122 bp. The 18srRNA were: forward,CCTGGATACCGCAGCTAGGA and reverse, GCGGCGCAATACGAATGCCCC; amplification length, 140 bp.The synthesized primers were purchased from Shenzhen Thermo Co., Ltd. (Shenzhen, China). The PCR products were subjected to electrophoresis on a 1.5% agarose gel and analyzed using a UV gel imaging analysis system. The relative expression levels of the target genes were calculated as the ratio of the absorbance of the target gene band to that of the internal control. Relative mRNA expression was quantified using the $2^{-\Delta\Delta Cq}$ method and normalized to the internal reference gene Gapdh.

2.4. Microarray data.

The data were screened and analyzed by two contributor using the following criteria for data analysis: i) The sample was homo sample; and ii) comparison was conducted between high levels of alpha-SMA in lung fibrosis and normal groups (negative control). Datasets GSE40839 and Datasets GSE53845 were acquired from the GEO (http://www.ncbi.nlm.nih.gov/geo; version 2.0) database for analysis (9, 10). In the GSE40839 and GSE53845 dataset, human sample were enriched with study. The probes were converted into the corresponding gene symbols according to annotation information provided by the platform.

2.5 Identification of DEGs.

DEGs were analyzed using GEO2R(http://www.ncbi.nlm.nih.gov/geo/geo2r; version 2.19.4), an online web tool that allows users to compare two or more datasets in a GEO series (11). We followed the methods of Wang et al(39). 2019.Probe sets without corresponding gene symbols or genes with > 1 probe set were averaged. Samples with an absolute value of log fold-change > 1 and $P < 0.05$ were considered DEGs.

2.6 Functional enrichment analysis.

To investigate the biological characteristics and functional enrichment of candidate DEGs, followed the methods of Wang et al(39), functional enrichment analysis was performed using Database for Annotation, Visualization and Integrated Discovery (https://david.ncifcrf.gov/; version 6.8). Results with $P < 0.05$ were considered significant. Additionally, Circos, a visualization software(version 0.1.1) for comparative genomics (12), was applied to identify overlapping genes from the input gene lists and shared GO terms, and a Venn diagram was plotted using an online tool (http://bioinformatics.psb.ugent.be/webtools/Venn/; version 1.0).

2.7 PPI network construction and module analysis.

A PPI network for DEGs was constructed using the Search Tool for the Retrieval of Interacting Genes (STRING) database (https://string-db.org/cgi/; version 11.0). As followed to the methods of Wang et al(39), interactions with a combined score of > 0.4 were considered significant. The results were visualized using Cytoscape software (version 3.7.1) (13). MCODE, a Cytoscape plugin, was used to identify the most significant module. The criteria for selection were as follows: MCODE score ≥ 3, degree cutoff = 2, node score cutoff = 0.2 and max depth = 100.

2.8 Statistical analysis.

Statistical analysis of all results was performed using SPSS 20.0 software. All data are presented as the mean ± SD. Significant differences between groups were determined using an unpaired Student's t-test. $P < 0.05$ was considered to indicate a statistically significant difference.

3. Result

3.1 Vitro Model of MRC-5 Cells Induced by PQ

The CCK-8 method was used to detect the toxicity and cell viability of PQ at different concentrations on MRC-5 cells. The results are shown in Fig. 1. In 48 hours, with the increase of PQ concentration, MRC-5 cells showed significant proliferation, MRC-5 cells proliferated significantly in 150 μmol / L of PQ. But over 48 h, the proliferation of MRC-5 cells was strongly inhibited. It can be seen that the highest non-lethal concentration of PQ is 200 μmol / L, and the time window is 48 h.

3.2 Western blot analysis

As shown in Fig. 2 and Table 1, western blot analysis resulted that collage I protein of PQ with concentrations of 200 μmol/L lasting 48 h was expression in the lung tissue. In addition, as shown in Fig. 3 and Table 2, western blotting demonstrated that PQ induced a pronounced increase in the protein expression levels of α-SMA, and the PQ with concentrations of 200 μmol/L lasting 48 h was highest expression of α-SMA.The results indicated the differentiation of lung fibroblasts into myofibroblasts. This differentiation process has been associated with lung fibrosis.

Table 1

Collage I and collage III protein expression in lung tissues detected by western blot analysis.

	1	2	3	4	5	6	7	8	9	10	11	12
COL I	881.3702	649.9987	1832.703	2568.678	2818.209	3147.572	3451.245	3181.307	3539.749	3513.014	3847.802	518
COL III	505.3061	484.2094	749.4388	908.0861	1260.177	1496.222	1701.527	1636.657	1462.328	1255.216	1323.994	179
GAPDH	4804.041	5780.667	5607.124	5567.676	5250.71	5264.191	5177.216	5562.457	5222.558	4894.892	4387.933	455

Table 2
PQ-induced α-SMA expression.

Sample	Repeat 1 Ct	Repeat 2 Ct	Repeat3 Ct	Mean Ct	ΔCT	ΔΔCT	$2^{-\Delta\Delta CT}$
1-SMA	28.73	28.68	28.61	28.67 ± 0.06	17.57 ± 0.15	0 ± 0.15	1 ± 0.1
2-SMA	28.28	28.36	28.85	28.5 ± 0.31	17.22 ± 0.16	-0.35 ± 0.16	1.27 ± 0.14
3-SMA	28.02	27.66	28.57	28.08 ± 0.46	16.96 ± 0.47	-0.61 ± 0.47	1.53 ± 0.49
4-SMA	27.73	27.62	27.77	27.71 ± 0.07	16.3 ± 0.07	-1.27 ± 0.07	2.41 ± 0.11
5-SMA	32.35	31.88	32.24	32.16 ± 0.25	14.95 ± 0.32	-2.62 ± 0.32	6.14 ± 1.35
6-SMA	27.85	27.78	27.94	27.85 ± 0.08	16.3 ± 0.12	-1.27 ± 0.12	2.42 ± 0.21
7-SMA	28.34	28.32	28.81	28.49 ± 0.28	17.34 ± 0.38	-0.23 ± 0.38	1.17 ± 0.29
8-SMA	27.16	27.23	27.17	27.19 ± 0.03	16.14 ± 0.22	-1.43 ± 0.22	2.7 ± 0.42
9-SMA	28.74	28.72	28.96	28.81 ± 0.13	17.26 ± 0.03	-0.31 ± 0.03	1.24 ± 0.03
10-SMA	28.92	28.84	28.70	28.82 ± 0.11	16.35 ± 0.14	-1.21 ± 0.14	2.32 ± 0.22
11-SMA	31.81	31.95	31.22	31.66 ± 0.39	17.1 ± 0.31	-0.47 ± 0.31	1.39 ± 0.31
12-SMA	32.17	31.68	32.28	32.04 ± 0.32	18.57 ± 0.28	1 ± 0.28	0.5 ± 0.1
13-SMA	30.86	30.40	30.01	30.42 ± 0.43	15.88 ± 0.41	-1.69 ± 0.41	3.23 ± 0.87
14-SMA	31.32	31.21	31.36	31.3 ± 0.08	14.14 ± 0.09	-3.43 ± 0.09	10.78 ± 0.7
15-SMA	26.73	23.48	25.61	25.27 ± 0.56	14.57 ± 0.15	0.02 ± 0.15	0.6 ± 0.1

1, control group was for 24 h;2, control group was for 48 h; 3,control group was for 72 h; 4, PQ with concentrations of 50 μmol/L was selected for 24 h; 5, PQ with concentrations of 50 μmol/L was selected for 48 h; 6, PQ with concentrations of 50 μmol/L was selected for 72 h; 7, PQ with concentrations of 100 μmol/L was selected for 24 h; 8, PQ with concentrations of 100 μmol/L was selected for 48 h; 9, PQ with concentrations of 100 μmol/L was selected for 72 h; 10, PQ with concentrations of 150 μmol/L was selected for 24h;11, PQ with concentrations of 150 μmol/L was selected for 48h; 12, PQ with concentrations of 150 μmol/L was selected for 72h; 13, PQ with concentrations of 200 μmol/L was selected for 24h; 14, PQ with concentrations of 200 μmol/L was selected for 48h; 15、PQ with concentrations of 200 μmol/L was selected for 72 h. tips: ΔCt=(target gene Ct −Internal reference Ct) Mean ± SE; ΔΔCt=(gene of interest in the test sampleΔCt −reference geneΔCt)Mean ± SE; Relative expression=($2^{-\Delta\Delta Ct}$)Mean ± SE.

3.3 Identification of DEGs in paraquat -induced human embryonic pulmonary fibrosis.

The microarray datasets GSE40839 and GSE53845 were standardized. The overlap between ontology terms associated with DEGs in GSE40839 and GSE53845 was high(Fig. 4); moreover, functional enrichment of these gene sets was analyzed together and 92 overlapping genes between the GSE40839 and GSE53845 datasets were identified (Fig. 4).

3.4 Functional enrichment analysis of DEGs.

Gene Ontology (GO) analysis identified that the DEGs were significantly enriched in components, including the'nucleic acid binding','CXCR chemokine receptor binding', 'cell surface', and'G-protein coupled receptor binding'(Table 3). In addition, biological processes and Kyoto Encyclopedia of Genes and Genomes (KEGG) pathway analyses demonstrated that the DEGs were enriched in pathways involved in the'TNF signaling pathway', 'Chemokine signaling pathway','Jak-STAT signaling pathway',and'p53 signaling pathway'(Table 3).

Table 3

Functional analysis of the hub genes identified from the protein-protein interaction network.

Term	Description	count	P-Value
GO:0003676	nucleic acid binding	26	0.0093558566
GO:0003700	transcription factor activity, sequence-specific DNA binding	14	0.0095883844
GO:0008083	growth factor activity	5	0.03424423
GO:0045236	CXCR chemokine receptor binding	3	0.020546538
GO:0001664	G-protein coupled receptor binding	5	0.03424423
GO:0001047	core promoter binding	4	0.027395384
GO:0000987	core promoter proximal region sequence-specific DNA binding	5	0.03424423
bta04668	TNF signaling pathway	10	0.027395384
bta04062	Chemokine signaling pathway	5	0.03424423
bta04630	Jak-STAT signaling pathway	4	0.027395384
bta04115	p53 signaling pathway	3	0.020546538

GO:Gene Ontology.

3.5 Module analysis from the PPI network.

Module analysis from the PPI network. The interactions of 92 DEGs were identified using the STRING online database. A PPI network was generated with Cytoscape, and the most significant modules were obtained using MCODE (Fig. 5A). AP-1 transcription factor subunit (JunB), fos-like antigen 2(FosL2), suppressor of cytokine signaling 3 (SOCS3), dual specificity phosphatase 1(DUSP1) ,C-C motif chemokine ligand 2 (CCL2) ,CCAAT/enhancer binding protein (CEBP),chemokine ligand 2 (CXCL2), activating transcription factor 3(ATF3) and CCAAT/enhancer binding protein (C/EBP)as hub genes (Fig. 5B). These genes were closely related to the term ‘transcription factor activity’ and were enriched in the ‘TNF signaling pathway’ (Table 3).

4. Discussion

Because PQ is highly toxic pesticide, and caused acute lung injury and subsequently develop pulmonary fibrosis, eventually it lead to respiratory failure and death(14). The main pathological changes associated with lung injury caused by PQ poisoning was that, Intranasal or oropharyngeal of PQ en-routed to lung casused oxidative damage imposed onto the alveolar cells thereby triggering the lung pathophysiology along with prodigious deposition of collagen onto the extracellular matrix, release of inflammatory cytokines, fibroblast proliferation etc(15, 16). However, the exact mechanisms of PQ-induced lung fibrosis remain largely unclear and no specific drugs for this disease have been approved. Thus, innovative treatment strategies are required to prevent, treat and even reverse pulmonary fibrosis which lied to PQ poisoning .

Importantly, this is the first study to report the preclinical vitro model of paraquat-induced pulmonary fibrosis and explore its potential mechanism though bioinformatics analysis. Pulmonary fibrosis is characterized by fibroblast proliferation and the abnormal accumulation of extracellular matrix (ECM) molecules, particularly fibrillar collagens(17, 18). Lung fibrosis-induced fibroblasts and myfibroblasts secrete more ECM, primarily collagen types I and III(19, 20), so the content of collagen in lung tissues can directly reflect the degree of pulmonary fibrosis. The extent of collagen deposition is reflected by the amount of Hyp content(21), and collagen deposition in local tissues can reflect the severity of pathology by collagen staining. Thus,in our study, we detected that in the PQ group after 200 mg/kg PQ poisoning lasting for 48 h, the collagen I and α-SMA were significantly upregulated expression. In another words, under PQ concentrations of 200 mg/kg, MRC-5 were severely pulmonary fibrosis.Thus, we found that PQ exposure significantly upregulated collage I,collage III and SAM expression in lung cells. These data indicated that PQ injury lung tissue, which activated the TNF signaling by recruiting inflammatory factor onto the lung cells, inline with the previous study(22).

Previous studies have demonstrated that TNF-α causes significant damages to lung tissues(23, 24), and are important regulators of the cell proliferation(25–27). Christopher et al. found that TNF-R2 can also independently activate JNK (c-jun N-terminal protein kinase) and ERK (extratracellular signal 2 regulated protein kinase) in lung tissue, indicating that TNF-R2 not only has "ligand transmission" Function, can also independently transmit signals(28).Paraquat can activate inflammatory cells such as macrophages and neutrophils to secrete a large number of inflammatory factors, and then participate in the occurrence of pulmonary fibrosis. Previous studies have suggested the levels of tumor necrosis factor α (TNF-α), nuclear factor (NF-κB), interleukin 1β (IL-1β) and IL-6 in experimental rats with acute lung injury and bronchoalveolar lavage fluid induced by paraquat(29). Nine hub genes (JUNB,FOSL2,SOCS3,DUSP1,CEBPB,CEBPD,ATF3,CCL2 and CXCL2) were identified as having the highest scores in the PPI network. JUNB,which is strongly dependent on the AP1 factor,could regulate collagen type 1 and collagen type II in pulmonary fibrosis(30).FOSL2 and SOCS3,that inhibited activation of signal transducers and activators of transcription 3 (STAT3) to promote fibroblast-to–myofibroblast transition, collagen release and fibrosis in vitro and in vivo(31).DUSP1,dual-specificity protein phosphatase-1, which aggravated the expression levels of collagen I, collagen IV, and fibronectin(32). CEBPB and CEBPD could act on bleomycin-induced fibrosis(33). ATF3 (activating transcription factor 3), a member of the integrated stress response (ISR), negatively regulates transcription of the PINK1 gene. ATF3 in type II lung epithelial cells accelerate mice from PQ-induced lung fibrosis(34). CCL2(chemokine ligand 2),which produced by AECs, promote fibrosis through CCR2 activation. CCR2 signaling is critical for the initiation and progression of pulmonary fibrosis, in part, through recruitment of pro-fibrotic bone marrow derived monocytes(35, 36).Chemokine receptor type 2 (CXCR2), which is a chemokine, which is highly

expressed in the lung, and exhibiting inflammatory and fibrotic effects(37). Therefore, TNF modulators had possibly potential as therapeutic targets in PQ-induced pulmonary fibrosis. The results of the present study revealed that the expression levels of JUNB,FOSL2,SOCS3,DUSP1,CEBPB,CEBPD,ATF3,CCL2 and CXCL2 were significantly higher in the lung fibrosis, and promoting pulmonary fibrosis(38).Thus, our findings may provide new insights into gene therapeuty in regulating the PQ-induced pulmonary toxicity.

5. Conclusion

Our findings firstly demonstrated that PQ-induced MRC-5 cells pulmonary fibrosis were successfully constructed preclinical vitro model in the highest non-lethal concentration of PQ is 200 μmol / L for 48h.Furthermore, we indicated that TNF singalong pathway and nine hub genes were possibly involved in PQ-induced lung fibrosis progression.Our study may aid in design of novel approaches for treating for control of PQ-induced pulmonary fibrosis.

Declarations

Conflict of interest

All authors have no conflicts of interest to declare.

Funding

The study was supported by grants from Guangdong Science and technology(nos. 2013B021800038), Foshan Science and technology(nos.2016AB002621) and Guangdong Medical Science and Techology Research Fund Project(nos. B2019103).

ETHICS APPROVAL AND CONSENT TO PARTICIPATE

Not applicable.

CONSENT FOR PUBLICATION

Not applicable.

AVAILABILITY OF DATA AND MATERIALS

The data used to support the findings of this study are available from the corresponding author upon request.

AUTHORS' CONTRIBUTIONS

ZXX and YM carried out the molecular research, drafted the manuscript. XCM and HJL participated in the the design of the study, GZC and XWG performed the statistical analysis. FY conceived of the study, and participated in its design and coordination and helped to draft the manuscript. All authors read and approved the final manuscript.

Acknowledgement

Not applicable.

Ethics approval and consent to participate

Not applicable.

Patient consent for publication

Not applicable.

References

1. Yu Youjia, Gao Zishan, Lou Jiaqian et al. Identification of Serum-Based Metabolic Feature and Characteristic Metabolites in Paraquat Intoxicated Mouse Models.[J] .Front Physiol, 2020, 11: 65-72.
2. Yin, Y., Guo, X., Zhang, S. L., and sun, C. Y. Analysis of paraquat intoxication epidemic (2002-2011) within China. *Biomed. Environ. Sci.* 2013, 26(6):509-512.
3. Suntres, Z.E. Role of antioxidants in paraquat toxicity. *Toxicology* 180, 2002, 180(1):65-77.
4. Hu, L., Yu, Y., Huang, H., Fan, H., Hu, L., Yin, C., et al. Epigenetic regulation of interleukin 6 by histone acetylation in macrophages and its role in paraquat-induced pulmonary fibrosis. *Front. Immunol. 2016,13(7*):696-670.
5. Chen J , Sun H , Zhang J . Analysis of long non-coding RNA expression profiles in Paraquat-induced pulmonary fibrosis[C]. Chinese Medical Association Emergency Medicine.2014,25(7):1-1.
6. Suman Patel, Kavita Singh, Seema Singh,etc. Gene Expression Profiles of Mouse Striatum in Control and Maneb + Paraquat-induced Parkinson's Disease Phenotype: Validation of Differentially Expressed Energy Metabolizing Transcripts[J]. Molecular Biotechnology, 2019,40(1):59-68.

7. Minling zhu, Xiankai Luo, Wencai Luo, et al. Endoplasmic Reticulum Stress and Autophagy are Involved in Paraquat Poisoning Induced Lung Injury[J]. Advances in Modern Biomedicine, 2018(2):254-258.
8. Ashutosh Kumar, Douglas Ganini, Ronald P. Mason. Role of cytochromecin α-synuclein radical formation: implications of α-synuclein in neuronal death in Maneb-induced and paraquat-induced model of Parkinson's disease[J]. Molecular Neurodegeneration, 2016,11(1):70-76.
9. Zhou X, Wu W, Hu H, Milosevic J et al. Genomic differences distinguish the myofibroblast phenotype of PQ-induced lung fibroblasts from airway fibroblasts. *Am J Respir Cell Mol Biol*2011 Dec;45(6):1256-62.
10. Junjie chen, hao sun, Jinsong zhang. Analysis of long non-coding RNA expression profiles in Paraquat-induced pulmonary fibrosis. Chinese Medical Association Emergency Medicine.2016,3(03):2-3.
11. Davis Sean,Meltzer Paul S,GEOquery: a bridge between the Gene Expression Omnibus (GEO) and BioConductor.[J] .Bioinformatics, 2007, 23: 1846-1857.
12. Yu Y , Ouyang Y , Yao W . shinyCircos: an R/Shiny application for interactive creation of Circos plot[J]. Bioinformatics, 2017,4(24):1229-1331.
13. Smoot Me, ono K, ruscheinski J, Wang Pl and ideker T: cytoscape 2.8: new features for data integration and network visualization. Bioinformatics ,2011,3(27): 431-432.
14. Yu, Yiming, Ouyang, Yidan, Yao, Wen. shinyCircos: an R/Shiny application for interactive creation of Circos plot[J]. Bioinformatics.2018,34: 1229-1231.
15. Smoot Michael E, Ono Keiichiro, Ruscheinski Johannes,etc. Cytoscape 2.8: new features for data integration and network visualization[J]. Bioinformatics, 2010,27: 431-432.
16. Guangju Z , Kaiqiang C , Changqin X , et al. Crosstalk between Mitochondrial Fission and Oxidative Stress in Paraquat-Induced Apoptosis in Mouse Alveolar Type II Cells[J]. International Journal of Biological Sciences, 2017, 13(7):888-900.
17. Murphy S , Lim R , Dickinson H , et al. Human Amnion Epithelial Cells Prevent Bleomycin-Induced Lung Injury and Preserve Lung Function[J]. Cell Transplantation, 2011, 20(6):909-923.
18. Fang He,Yuying Wang,Yuxiang Li et al. Human amniotic mesenchymal stem cells alleviate paraquat-induced pulmonary fibrosis in rats by inhibiting the inflammatory response.[J] .Life Sci., 2020, 243: 1-28.
19. Bocchino Marialuisa,Agnese Savina,Fagone Evelina et al. Reactive oxygen species are required for maintenance and differentiation of primary lung fibroblasts in idiopathic pulmonary fibrosis.[J] .PLoS ONE, 2010, 5: e14003:1-11.
20. Baum, J., and Duffy, H. S. Fibroblasts and myofibroblasts: what are we talking about? Cardiovasc. Pharmacol.2011, 57 (4), 376–379.
21. Boyapally Raju,Pulivendala Gauthami,Bale Swarna et al. Niclosamide alleviates pulmonary fibrosis in vitro and in vivo by attenuation of epithelial-to-mesenchymal transition, matrix proteins & Wnt/β-catenin signaling: A drug repurposing study.[J] .Life Sci., 2019, 220: 8-20.
22. Li Gui-Ping,Yang Hao,Zong Shao-Bo et al. Diterpene ginkgolides meglumine injection protects against paraquat-induced lung injury and pulmonary fibrosis in rats.[J] .Biomed. Pharmacother., 2018, 99: 746-754.
23. A.B. Lipke, G. Matute-Bello, R. Herrero, K. Kurahashi, V.A. Wong, S.M. Mongovin, T.R. Martin, Febrile-range hyperthermia augments lipopolysaccharide-induced lung injury by a mechanism of enhanced alveolar epithelial apoptosis, J. Immunol. 2010 184 (7) 3801–3813.
24. R. Malaviya, J.D. Laskin, D.L. Laskin, Anti-TNFα therapy in inflammatory lung diseases, Pharmacol. Ther. 2017,10 (20) :90–98.
25. K.A. Stern, T.L. Place, N.L. Lill, EGF and amphiregulin differentially regulate Cbl recruitment to endosomes and EGF receptor fate, Biochem. J. 2008,410 (3): 585–594.
26. R. Avraham, Y. Yarden, Feedback regulation of EGFR signaling: decision making by early and delayed loops, Nat. Rev. Mol. Cell Bio. 2011,12 (2): 104–117.
27. F. Van Herreweghe, N. Festjens, W. Declercq, P. Vandenabeele, Tumor necrosis factor-mediated cell death: to break or to burst, that's the question, Cell. Mol. Life Sci.2010, 67 (10): 1567–1579.
28. Christopher R, Blanche S , Venkat akrishna S.Tumor necrosis fact or 2 induced activation of c-Jun N-teminal kinase is mediated by TRAF2[J] .EMBO J , 1997 , 16(5):1080-1092.
29. Perfluorocarbon attenuates inflammatory cytokines, oxidative stress and histopathologic changes in paraquat-induced acute lung injury in rats[J]. Environmental Toxicology & Pharmacology, 2016, 42:9-15.
30. Papaioannou Ioannis,Xu Shiwen,Denton Christopher P et al. STAT3 controls COL1A2 enhancer activation cooperatively with JunB, regulates type I collagen synthesis posttranscriptionally, and is essential for lung myofibroblast differentiation.[J] .Mol. Biol. Cell, 2018, 7(29): 84-95.
31. Dees Clara,Pötter Sebastian,Zhang Yun et al. TGFβ-induced epigenetic deregulation of SOCS3 facilitates STAT3-signaling to promote fibrosis.[J] .J. Clin. Invest., 2020, undefined: undefined.
32. Ge Yanni,Wang Juan,Wu Dengke et al. lncRNA NR_038323 Suppresses Renal Fibrosis in Diabetic Nephropathy by Targeting the miR-324-3p/DUSP1 Axis.[J] .Mol Ther Nucleic Acids, 2019, 17: 741-753.
33. Satoh Takashi,Nakagawa Katsuhiro,Sugihara Fuminori et al. Identification of an atypical monocyte and committed progenitor involved in fibrosis.[J] .Nature, 2017, 541: 96-101.
34. Wu Chaochen,Lin Haobo,Zhang Xiao,Inhibitory effects of pirfenidone on fibroblast to myofibroblast transition in rheumatoid arthritis-associated interstitial lung disease via the downregulation of activating transcription factor 3 (ATF3).[J] .Int. Immunopharmacol., 2019,2(74): 105700.
35. Bueno Marta,Brands Judith,Voltz Lauren et al. ATF3 represses PINK1 gene transcription in lung epithelial cells to control mitochondrial homeostasis.[J] .Aging Cell, 2018, 17(1):1-13.
36. Yang Jibing,Agarwal Manisha,Ling Song et al. Diverse Injury Pathways Induce Alveolar Epithelial Cell CCL2/12 Which Promotes Lung Fibrosis.[J] .Am. J. Respir. Cell Mol. Biol., 2020, 10(10):1-44.

37. Xue Mingshan,Guo Zijun,Cai Chuanxu et al. Evaluation of the Diagnostic Efficacies of Serological Markers KL-6, SP-A, SP-D, CCL2, and CXCL13 in Idiopathic Interstitial Pneumonia.[J] .Respiration, 2019, 98: 534-545.
38. Zhang Hua-Wei,Wang Qian,Mei Hong-Xia et al. RvD1 ameliorates LPS-induced acute lung injury via the suppression of neutrophil infiltration by reducing CXCL2 expression and release from resident alveolar macrophages.[J] .Int. Immunopharmacol., 2019, 76: 105877.
39. Wang Jiao,Liu Honghong,Xie Guijiao et al. Identification of hub genes and key pathways of dietary advanced glycation end products-induced non-alcoholic fatty liver disease by bioinformatics analysis and animal experiments.[J] .Mol Med Rep, 2020, 21: 685-694.

Figures

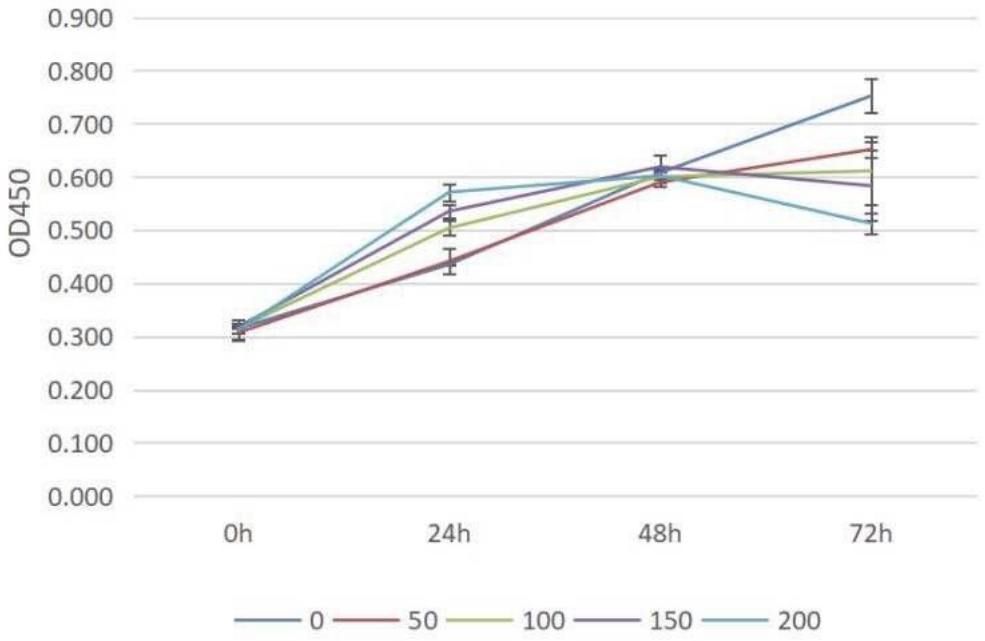

Figure 1

cell viability of PQ at different concentrations on MRC-5 cells by CCk-8 assay.

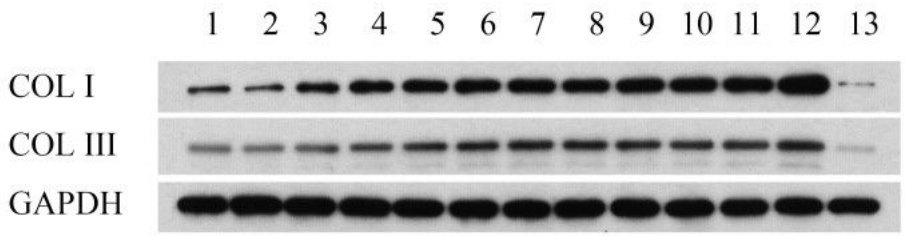

Figure 2

Collage I and collage III protein expression in lung tissues detected by western blot analysis. Lane 1, control group; lane 2, PQ with concentrations of 50 μmol/L was selected for 24h; lane 3, PQ with concentrations of 50 μmol/L was selected for 48h; lane 4, PQ with concentrations of 50 μmol/L was selected for 72h; lane 5, PQ with concentrations of 100 μmol/L was selected for 24h; lane 6, PQ with concentrations of 100 μmol/L was selected for 48h; lane 7, PQ with concentrations of 100 μmol/L was selected for 72h; lane 8, PQ with concentrations of 150 μmol/L was selected for 24h；lane 9, PQ with concentrations of 150

μmol/L was selected for 48h，lane 10, PQ with concentrations of 150 μmol/L was selected for 72h，lane 11, PQ with concentrations of 200 μmol/L was selected for 24h，lane 12, PQ with concentrations of 200 μmol/L was selected for 48h，lane 12, PQ with concentrations of 200 μmol/L was selected for 72h.

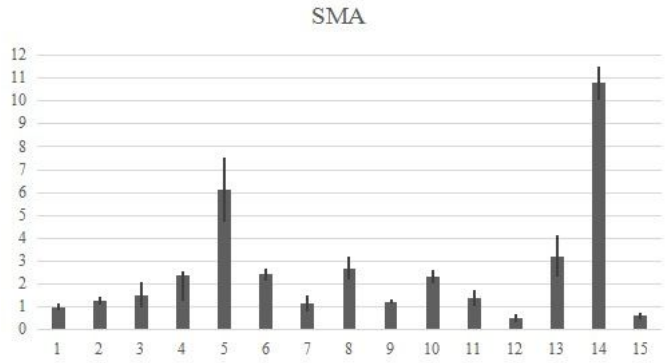

Figure 3

PQ-induced α-SMA expression. 1, control group was for 24h;2, control group was for 48h; 3，control group was for 72h; 4, PQ with concentrations of 50 μmol/L was selected for 24h; 5, PQ with concentrations of 50μmol/L was selected for 48h; 6, PQ with concentrations of 50μmol/L was selected for 72h; 7, PQ with concentrations of 100μmol/L was selected for 24h; 8, PQ with concentrations of 100 μmol/L was selected for 48h; 9, PQ with concentrations of 100 μmol/L was selected for 72h; 10, PQ with concentrations of 150 μmol/L was selected for 24h，11, PQ with concentrations of 150μmol/L was selected for 48h，12, PQ with concentrations of 150 μmol/L was selected for 72h，13, PQ with concentrations of 200 μmol/L was selected for 24h，14, PQ with concentrations of 200 μmol/L was selected for 48h，15，PQ with concentrations of 200 μmol/L was selected for 72h.

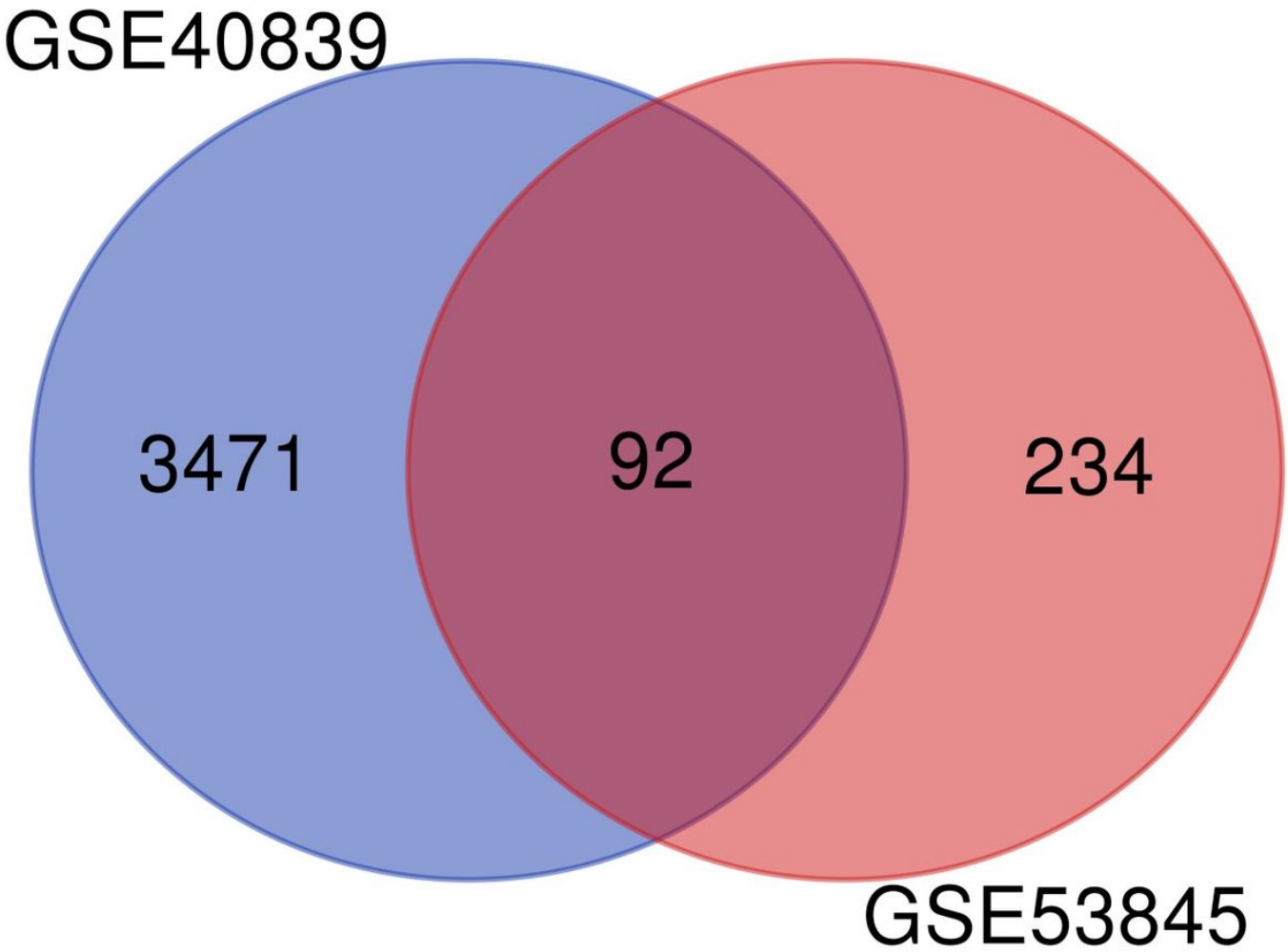

Figure 4

Venn diagram of DEGs in the two GEO datasets.

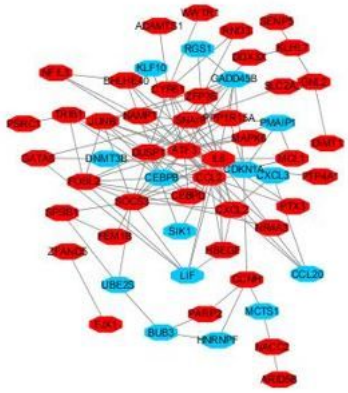

(A)

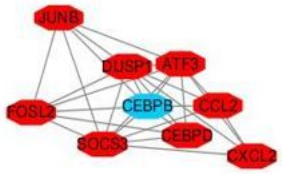

(B)

Figure 5

Module analysis of the PPI network. Up-regulated genes are marked in light red, down–regulated genes are marked in light blue（A). The most significant module generated from the PPI network. JUNB, FOSL2, SOCS3,DUSP1, CCL2,CEBPD, CXCL2,ATF3 protein-protein interaction(B).Up-regulated genes are marked in light red, down–regulated genes are marked in light blue.